Efficiency Enhancements to a Linear AC Voltage Regulator: Multi-Winding versus Multi-Transformer Design

Priyanwada Nimesha Wijesooriya, *Student Member, IEEE*, Nihal Kularatna, *Senior Member, IEEE*, and D. Alistair Steyn-Ross

***Abstract*— Electricity distribution companies are required to supply electric power, which conforms to accepted standards, that place limits on voltage fluctuations beyond nominal values. However, it is common for these fluctuations to exceed the specified standards. One solution to this problem is to install stand-alone RMS voltage regulators at the consumer site. Commonly available AC regulators typically have limitations such as slow response time, flattened sine wave output, low efficiency, and limited operating range.**

The linear AC voltage regulator is a relatively new type of solid-state, single-phase AC regulator for consumer-end, which addresses most of the above issues. It is based on a series transistor-array coupled with a line-frequency transformer that works seamlessly from boost-to buck-mode in the range of $0.8 - 1.1$ per-unit values of line voltage, without a need of any transformer configuration changes. However, previous prototypes exhibited reduced efficiency when the line voltage exceeded the nominal value. This paper presents two alternative designs that achieve efficiencies of $90 - 95\%$, usually required in commercial implementation. Analytical and experimental results of a multi-winding versus multi-transformer based prototypes of 300 VA output capacity are presented.

***Index Terms*— power conditioners, efficiency, power semiconductor array, RMS AC voltage regulation, solid state regulators, transformers**

I. Introduction

THE quality of power is a significant factor that determines the performance of electrical devices [1, 2]. Increasing demand for electricity and proliferation of electronic devices create power line disturbances which affect the waveform fidelity and degrade the power quality [1, 3].

RMS voltage variation is a common power quality phenomenon seen at the consumer end [1, 3]. According to the definition in IEEE Std. 1159-2019 regarding recommended practice for monitoring electric power quality, RMS voltage variations can be categorized as voltage dips, swells, over-voltages and under-voltages depending on the magnitude and duration of occurrence, which is summarized in Fig. 1 [3]. The aftermath of voltage variations is lower device efficiency, malfunction or reduced life-span of electric equipment and unexpected system shut-down [1, 2]. To mitigate the RMS voltage variations, AC voltage regulators can be connected at the consumer-end to achieve a constant voltage supply at the premises [1].

The patented linear AC voltage regulator described in reference [4, 5] is a new member of the AC voltage regulator family. However, in developing it into a commercial prototype, the base technique needs to be modified to achieve competitive efficiency levels compared to traditional RMS voltage regulators. The objective of this paper is to present the implementation details of two proposed solutions for efficiency enhancement of this technique, (i) multi-transformer regulator [6] and (ii) multi-winding transformer regulator [7], including analytical and experimental results validated by simulations. The remainder of this introductory section describes the motivations that led to the invention of the linear AC regulator and its weaknesses that were addressed in the commercial prototype, which is currently under development.

A. A Summary of RMS AC Voltage Regulators

The following paragraphs describe the significant drawbacks of the commercially available AC voltage regulators.

Servo-driven variacs are bulky and slow to respond due to their mechanical structure employing a servo mechanism to continually adjust the turns ratio of an autotransformer for voltage regulation [8, 9]. In *ferro-resonant regulators*, the transformer operation in the saturation region is less efficient and results in a clipped sinusoidal output [10]. *Transformer tap changers* utilizes contactors or mechanical relays for tap switching, which may trigger arcing across taps if the input

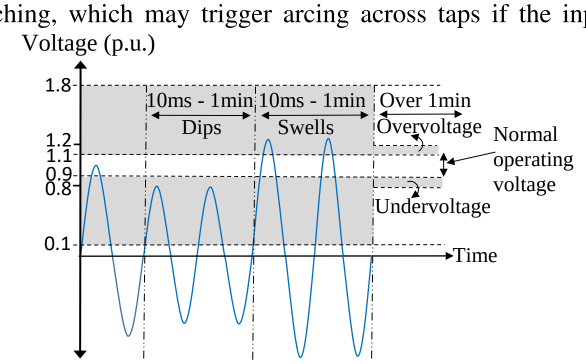

Fig. 1: Definition for RMS voltage variations [3]

Manuscript submitted for review on 13/01/2020. The authors gratefully acknowledge the financial support by a Kiwinet commercial research grant to carry out this work. They are also very thankful to Thor Technologies, Perth, Australia for their collaborative support, and for the opportunity to propose significant modifications to improve an existing commercial power quality product.

School of Engineering, University of Waikato, Hamilton 3240, New Zealand(e-mail: nimesha.diyadawa@gmail.com).
(e-mail: nihal.kularatna@waikato.ac.nz)
(e-mail: asr@waikato.ac.nz)

line voltage fluctuates rapidly [11, 12].

Solid-state regulators are compact and energy-efficient devices that use thyristors or IGBTs under different operational principles discussed in [13–18]. In thyristor-based AC-AC regulators, the commutation problem is a major drawback that causes voltage spikes for inductive loads [13]. Electronic transformers and DC-to-AC inverter-based regulators use PWM technique for selective switching based on current/voltage waveforms. This high-frequency operation introduces harmonics and RFI/EMI related defects at the output waveform, which requires RFI/EMI suppression for EMC compliance. These additional filter circuits contribute to higher losses and lower efficiency while the use of voltage/current sensors increases the price and the complexity of the device [13, 15]. Besides, the majority of solid-state designs can only regulate either in boost or buck mode, which is a common limitation discussed in [13–16, 19], that may limit the usage of such products.

Given the above summary on commercial RMS voltage regulators, none of them are well-positioned for worst-case power quality situations seen in most of the developing countries due to infrastructure limitations, as discussed in [20, 21].

Linear AC regulation technique was originally developed to overcome the typical issue of a flattened sine wave in a ferro-resonant regulator and the slow response time of servo-driven variacs. Although, the linear technique is based on a continually varying AC impedance generated by a power transistor array it does not create the typical RFI/EMI issues common to switching type solid-state regulators.

Work related to this article was motivated by the request of a commercial PQ products manufacturer who has already introduced a commercial 2 kVA AC regulator of the servo-driven variac type where the speed of response was low around $1.5 - 2$ s. Although a solid-state regulator based on a high-frequency PWM type switching could achieve theoretical 100% efficiency, their real-world efficiency falls within $85 - 90\%$ [14, 16]. Alternatively, in a ferro-resonant type regulator, approximately $200 - 250$W could be wasted for every kilowatt delivered to the load giving similar efficiencies. This situation will be further deteriorated with a precisely set air gap, which adds to the weight and the cost.

Given the above consideration, authors were motivated to extend the patented linear AC regulator technique onto this commercial project with the task of further improving its limitations of inadequate efficiency, while achieving a faster speed of response and a lower cost design based on 50 Hz transformer at the core of the design.

The structure of this paper is as follows: Section II discusses the basics of the linear AC technique and its significant weaknesses. Two alternative solutions for efficiency enhancement are proposed in Section III. Section IV presents an equivalent circuit model for the two proposed solutions. Simulation and experimental results are discussed in Section V and Section VI brings the conclusion.

II. Essentials of the Linear AC Technique

Patented linear AC regulator was developed in the late 1980s' as a solution to the severe AC voltage variations in developing countries like Sri Lanka.

The target set by the commercial partner was to prove that the linear technique can be further improved to reach the efficiencies of high-frequency PWM types, while the assembly cost of the product to be lower than a servo-driven or a PWM type. Here the criteria were to prove that having a modified version of a simple 50 Hz transformer at the centre of the design, the end to end efficiency could be reached closer to the transformer's efficiency, in a commercial implementation for mass-scale manufacture.

Fig. 2(a) indicates the key concept of the patented linear AC regulator based on a simple two-winding, a line-frequency transformer which provides a seamless buck and boost voltage at the secondary winding, which is in series with the input supply and the output load. Variable impedance, Z_{series} is connected between points A and B of the power stage to vary the effective impedance in relation to input voltage variations. Analogue design concepts related to this technique are presented in detail in [22].

The overall operation of the power stage is based on the control of Z_{series} over a wide range of resistances from near zero to near infinity similar to linear DC regulators where the series power transistor acts as a variable resistor taking care of the input to output voltage difference. As shown in Fig. 2(b), the BJT array is placed within bridge points of a rectifier bridge to eliminate voltage reversal across the power transistors. Traditional feedback control is implemented to monitor the output AC voltage and convert that to an equivalent DC value using an RMS/DC converter IC. This equivalent DC voltage is compared with a reference DC value and using an optoisolator based drive stage and it continually keeps adjusting the impedance of a series BJT array. Key elements of the feedback controller is shown in Fig. 2(c).

A. Implementation Aspects of the Variable AC Impedance

Developing an electronically-variable AC impedance (Z_{series}) as in Figure 2(a), comes with several significant challenges:

(a) Z_{series} should be an AC impedance which could vary from near-zero ohms to near-infinite value
(b) Z_{series} needs to withstand several hundred volts (based on 230 V, 50 Hz nominal AC input)
(c) Necessity to keep the feedback loop electronically isolated from the power stage, for safety and reliability.

Figure 2(d) depicts how the value of Z_{series} is continually varied with a feedback signal provided by an electrically isolated control unit. This electrical isolation is provided through a set of optoisolators, as indicated in Figure 2(e), for easy implementation of low voltage control circuits with significant reliability required in commercial product implementation. Z_{series} can be implemented by an array based on any power semiconductors such as BJTs, MOSFETs or IGBTs. A method of emulating a variable impedance using power BJTs is discussed in the previous work [4, 5, 22].

When the input voltage keeps on rising towards the highest worst-case scenario, ranging from 180 V to 250 V, a constant output voltage is maintained by increasing the array voltage from 0 to $370\sqrt{2}$ V; thus, an array of power semiconductors is used to withstand such high voltages [4, 22].

Following Figure 2(d), a high voltage across the bridge points of the transistor array can be equally distributed among several series connected transistors by suitably adjusting R_{B1} to R_{Bm} values, while the voltages across each transistor is kept approximately equal [4, 5, 22]. Thus, for an array of m-elements, if transistors have a constant current gain of h_{FE}, $i_{\text{C}} = h_{\text{FE}} i_{\text{B}}$, the effective resistance, $Z_{\text{CE}}(t)$ between the transistor collector and emitter is given by

$$R_{\text{CE}} = Z_{\text{array}} \approx m\frac{R_{\text{B}}}{h_{\text{FE}}}\left(1+\frac{i_{\text{x}}}{i_{\text{B}}}\right) \quad (1)$$

where the individual base resistances (assuming equal voltages across transistors) are related as follows,

$$R_{\text{B1}} = \frac{R_{\text{B}}}{m}; R_{\text{B2}} = \frac{R_{\text{B}}}{m-1}; R_{\text{B3}} = \frac{R_{\text{B}}}{m-2}; ..; R_{\text{Bm}} = R_{\text{B}} \quad (2)$$

v_{CE} - collector-emitter voltage (array voltage)
v_{BE} - base-emitter voltage
i_{C} - instantaneous collector current
i_{B} - instantaneous base current
i_{x} - diverted portion of the base current by the opto-transistor
R_{B} - external resistance between base and collector

Two extreme cases of the resistance across the power transistor R_{CE}, are such that close to zero (by short circuit base-collector junction) and infinite (by short circuit base-emitter junction). Based on (1), the effective collector–emitter resistance can be controlled by varying either R_{B} or i_{x}. The optotransistor between base and emitter controls i_{x} thus setting the $i_{\text{x}}/i_{\text{B}}$, the base-current diversion ratio. Darlington pairs are used to maintain an adequate gain for each transistor.

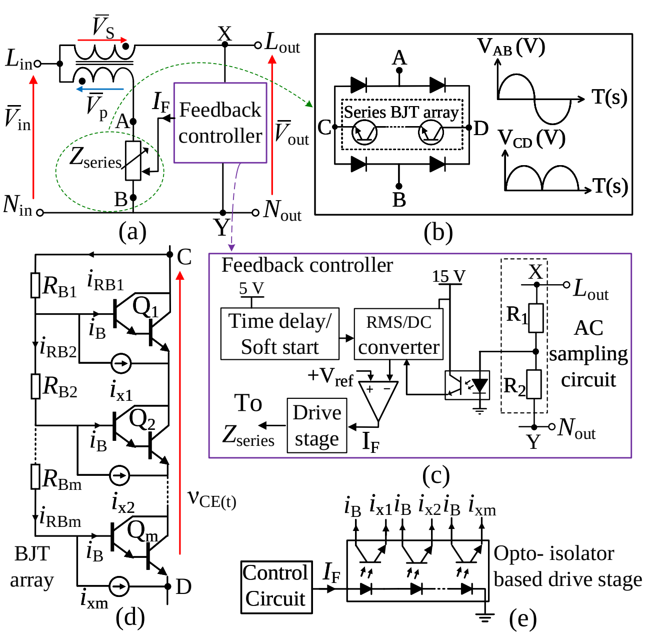

Fig. 2: Block diagrams of the linear AC regulator circuit blocks (a) basic implementation of the regulator (b) variable AC impedance; (c) feedback controller; (d) series transistor array; (e) optoisolator based driver unit

B. Boost – Buck Capability by Transistor Impedance Variation

As discussed above, this technique employs a line-frequency transformer with two windings (a primary and a secondary) where the transistor array is connected in series to the primary winding, as illustrated in Figure 3. One significant advantage of this design is that it allows boost and buck control without any physical change of the transformer winding configuration [4, 22]. This section briefs the boost and buck operation of this unique design.

According to Figure 3(a), based on an ideal transformer with a turns ratio of $n:1$ (primary to secondary), the relationship between the load current ($\overline{I}_{\text{L}}$) and the primary current ($\overline{I}_{\text{p}}$) is given by $\overline{I}_{\text{p}} = \overline{I}_{\text{L}}/n$ [22]. If $\overline{V}_{\text{s}}$ and $\overline{V}_{\text{p}}$ are primary and secondary RMS voltages respectively, the relationship of the winding voltages can be written as $\overline{V}_{\text{p}} = n\overline{V}_{\text{s}}$.

For any general load connected to the regulator output, assuming an ideal transformer, the following approximate equation gives the relationship between the input, output and array voltages in terms of transformer turns ratio,

$$\overline{V}_{\text{out}} = \overline{V}_{\text{in}}(1+1/n) - \overline{I}_{\text{L}} R_{\text{a}}/n^2 \quad (3)$$

When the input voltage is below nominal ($\overline{V}_{\text{in}} < \overline{V}_{\text{out}}$), as shown in Fig. 3(a), the control circuit drives the array and manipulates the transformer primary winding to induce a secondary voltage that maintain a constant output voltage. Table I presents basic transformer relationships.

The phaser diagram in Fig. 3(a) illustrates the regulation in boost mode. Here we assume the load current ($\overline{I}_{\text{L}}$) is lagging the input voltage ($\overline{V}_{\text{in}}$) by an angle ϕ. If the array impedance is purely resistive and the transformer is ideal, based on (3), the regulator can maintain a constant $\overline{V}_{\text{out}}$ within the arc TT' of the circle with radius $|\overline{V}_{\text{out}}|$ [20]. For a given transformer turns ratio, n, the boundaries of the regulation region are the two tangential points, T and T' of the worst case load phase angles of $\pm\phi_{\max}$.

Fig. 3(b) illustrates buck-mode regulation. When the input voltage rises above nominal ($\overline{V}_{\text{in}} > \overline{V}_{\text{out}}$), the required bucking voltage is induced in the secondary by manipulating the transistor array into a very high impedance. High voltage across the array forces a reversal of the voltage polarity of the transformer windings. Refer Table I for basic transformer relationships.

C. Drawbacks of the original linear AC technique

Fig. 4 shows the efficiency data extracted from [22] of the first linear-regulator prototype of 5 A load current capacity, compared with a recent low-current version based on the same transformer configuration as illustrated in Figs. 3(a) and (b). As indicated by the graphs, these prototypes are able to operate

TABLE I: Basic relationships of the linear AC regulator

Boost mode	Buck mode
$\overline{V}_{\text{out}} = \overline{V}_{\text{in}} + \overline{V}_{\text{s}}$ $\overline{V}_{\text{in}} = \overline{V}_{\text{p}} + \overline{V}_{\text{a}}$	$\overline{V}_{\text{out}} = \overline{V}_{\text{in}} - \overline{V}_{\text{s}}$ $\overline{V}_{\text{in}} = \overline{V}_{\text{a}} - \overline{V}_{\text{p}}$
$\overline{V}_{\text{a}} = \overline{I}_{\text{p}} Z_{\text{a}}$	

This article has been accepted for publication in a future issue of this journal, but has not been fully edited. Content may change prior to final publication. Citation information: DOI 10.1109/JESTIE.2020.3003350, IEEE Journal of Emerging and Selected Topics in Industrial Electronics

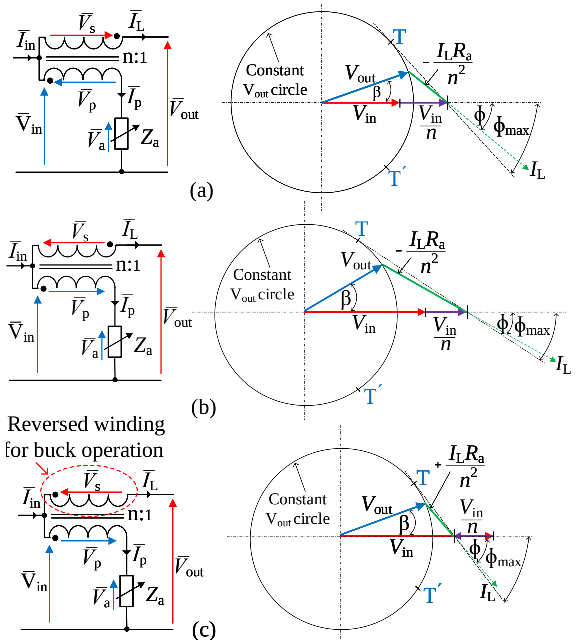

Fig. 3: Schematic and phaser diagrams of linear AC regulator (a) boost-mode; (b) buck-mode; (c) an alternative transformer configuration for buck operation.

bi-directionally over a wide range of input voltages from 180 V to 250 V (first prototype- 160 V to 250 V) allowing a regulation at 230 VAC [22]. As shown in the graphs, the efficiency is reduced at higher input voltages due to increasing array losses when driven into high impedance. Note that the efficiency graphs do not start from the same point due to the different turns ratios of the transformers utilized for the two different prototypes.

An alternative configuration to eliminate the extra losses in the transistor array when the input voltage exceeds the nominal voltage is shown in Fig. 3(c). The two terminals of the secondary winding switched, contrary to the configuration demonstrated in Fig. 3(a) and (b); therefore the polarity of the induced secondary voltage is applied to the opposite direction, in a subtractive manner, compared to the polarity indicated in Fig. 3(a) [23, 24]. This winding arrangement allows the transformer to produce a subtractive voltage required to regulate in buck mode without driving the array into high impedance. However, this requires a set of AC switches to change the configuration to a reversed-secondary winding. This principal has been improved into commercially viable solutions for efficiency enhancement to the linear regulator and presented in detail in Section 3.

In the prototype discussed above, the turns ratio of the transformer is set to $180/50$ to ensure maximum efficiency at the worst case input voltage of 180 V by driving the transistor array into saturation. The condition for maximum efficiency at the minimum input voltage is given by (3) where the array is driven into saturation so that the array impedance approaches zero. Thus, the minimum input voltage is $\overline{V}_{\text{in}}^{\text{min}} = n\overline{V}_{\text{out}}/(n+1)$ for which the power dissipation across the array is minimum. If $\overline{I}_{\text{out}} = \overline{I}_{\text{L}}$, and $\overline{I}_{\text{in}} = \overline{I}_{\text{L}} + \overline{I}_{\text{p}}$ the overall efficiency (η) of the regulator can be written as,

$$\eta = \frac{n\overline{V}_{\text{out}}}{(n+1)\overline{V}_{\text{in}}} \tag{4}$$

Thus, for a constant output voltage, (4) shows the dependence of the optimum regulator efficiency on the transformer turns ratio (n) at any input voltage.

In a situation where the input voltage reaches nominal voltage level of 230 V, the correction voltage given by the secondary should be zero. To facilitate this, the control unit adjusts the quantity, $R_{\text{a}}\overline{I}_{\text{L}}/(n^2) = 230\times 50/180$ (for a resistive load), from which the voltage at the primary side ideally becomes zero. One disadvantage of this particular situation is that when the input line voltage is 230 V (so does not need regulation) the above prototype still dissipates power in the array, thus diminishing the efficiency as indicated in Fig. 4 [4, 22].

The relationship between the device output power ($\overline{V}_{\text{out}}\overline{I}_{\text{L}}$) and the array power dissipation ($\overline{V}_{\text{a}}\overline{I}_{\text{p}}$) can be simplified into,

$$\frac{P_{\text{array}}}{P_{\text{out}}} = \frac{\overline{V}_{\text{in}}(n+1) - n\overline{V}_{\text{out}}}{n\overline{V}_{\text{out}}} \tag{5}$$

Assuming a constant output voltage and current, and a fixed transformer turns ratio, the above equation implies that as the input voltage increases, array losses become more significant.

In summary, the basic linear AC regulator is a good replacement for commonly used saturating ferro-resonant regulators and slow responding servo-driven variacs. However, for a commercial application, its low efficiency at higher input voltages needs to be addressed. This motivates alternative design strategies aimed at efficiency enhancement for higher input voltages based on following two approaches:

- multi-transformer [6]
- multi-winding single transformer [7]

The essentials of these alternative approaches are described below.

III. Proposed Solutions to Enhance Efficiency of the Linear AC Regulator

A. Implementation of a Series Multiple-Transformer Regulator

The original technique discussed in Section II have the advantage of one single transformer configuration without any tap changes or configuration changes. However, when the input voltage rises above the nominal, larger heat sinks are required, which increases the cost of the commercial product.

To achieve voltage-bucking capability with the transistor array operating at lower voltage for good efficiency, we could use two transformers which comes into operation alternatively [6]. This is the case of combining the configurations in Fig. 3(a) and (b).

Fig. 5(a) shows a possible solution that employs two series-connected low-power transformers in which the primary windings are connected in series with two transistor arrays controlled by a feedback circuit. During the change-over from boost to buck, the active regulation shifts from one transformer to the other, with the transformer windings being configured to induce voltages of opposite polarities to allow for boost or buck action [6]. This eliminates the requirement for driving the transistor array into very high impedance, hence minimizing the significant power losses during buck regulation.

Fig. 5(b) and (d) illustrates the transformer utilization for boost- and buck-mode regulation with optimum efficiency. The change-over between two transformers is done using switch S-2. Fig. 5(c) indicates a method that bypasses the regulating circuit using switch S-1, when the input voltage falls within a $\pm 2\%$ tolerance level ($V_{\text{in}} = 225 - 235$ V) of nominal voltage. This will prevent array dissipating power unnecessarily at the input voltage range falls within the accepted level of nominal voltage, avoiding the drop in device efficiency shown in Fig. 4. Switches S-3 and S-4 are used to disconnect the transistor arrays from the current loop whenever they are not in use. This disconnection is required to eliminate unnecessary power dissipation due to leakage currents in the Darlington pair, when they are in cut-off mode where a maximum voltage appears across the array.

The transformer turns ratios are selected for optimum efficiency at the worst case input voltages given by the following relationship for a nominal output of 230 VAC,

$$\left(1 - \frac{1}{n+1}\right)\overline{V}_{\text{out}} \leq |\overline{V}_{\text{in}}| \leq \left(1 + \frac{1}{n+1}\right)\overline{V}_{\text{out}} \quad (6)$$

As in Fig. 5, if the induced secondary voltages are $\overline{V}_{\text{s1}}$ and $\overline{V}_{\text{s2}}$, the regulated output is given by,

$$\overline{V}_{\text{out}} = \overline{V}_{\text{in}} + \overline{V}_{\text{s1}} \pm \overline{V}_{\text{s2}} \quad (7)$$

The ($\pm$) sign denotes the voltage polarity induced in the windings of transformer-2. Other basic relationships between the transformer parameters and the array voltages are,

$$\overline{V}_{\text{in}} = \overline{V}_{\text{p1}} + \overline{V}_{\text{a1}} \quad (8)$$

$$\overline{V}_{\text{in}} + \overline{V}_{\text{s1}} \pm \overline{V}_{\text{p2}} = \overline{V}_{\text{a2}} \quad (9)$$

Assuming an ideal transformer with no flux leakage or winding resistances, the output of the dual-transformer based approach is given by,

$$\overline{V}_{\text{out}} = \overline{V}_{\text{in}}\left(1 + \frac{1}{n_1}\right)\left(1 - \frac{1}{n_2}\right) + \left(\frac{1}{n_2^2} - 1\right)\frac{\overline{I}_{\text{L}}}{n_1^2}Z_{\text{a1}} + \frac{\overline{I}_{\text{L}}}{n_2^2}Z_{\text{a2}} \quad (10)$$

In terms of input/output voltages and the turns ratios, the regulator efficiency can be simplified as below,

$$\eta = \frac{n_1 n_2 \overline{V}_{\text{out}}}{(n_1 + 1)(n_2 - 1)\overline{V}_{\text{in}}} \quad (11)$$

Due to the lower cost, availability and easy mass-scale manufacturing of standard low-power transformers, the dual-transformer approach is an economical solution for achieving a good overall efficiency. However, in a commercial product, requiring two separate transformers is not optimal due to practical issues such as transformer-beating. Hence the commercial partner of this project required the research team to consider a single-transformer solution for efficiency improvements.

B. Implementation of a Multiple-Winding Transformer Regulator

In order to eliminate the constraints of the dual-transformer approach while achieving an efficiency enhancement, a novel approach using a single transformer was introduced [7]. This technique employs a step-down transformer with two distinct primary windings which are able to induce voltages of opposite polarities in the secondary for boost and buck regulation, as indicated in Fig. 6(a). To manipulate the two primary windings independently, separate transistor arrays are connected in series with each winding. Fig. 6(b), (c) and (d) illustrate the winding utilization to achieve optimum efficiency over a wide range of input voltages.

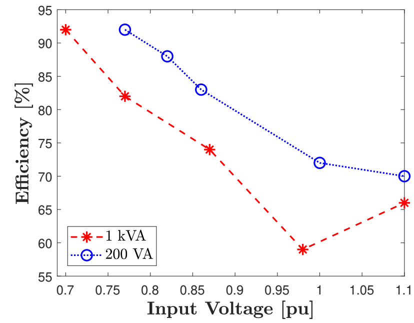

Fig. 4: Efficiency vs input line voltage from prototypes based on a single-transformer of two-windings configuration for 1 A load current. Transformer turns ratios are $n_{\text{red},*} = 160/70$, $n_{\text{blue,o}} = 180/50$. ($*$ graph is adapted from [22])

For a toroidal transformer with three windings of which the number of turns of primary-1, primary-2 and secondary are N_1, N_2 and N_3 respectively, Ampere's law suggests that the net magneto-motive force of the transformer core will be zero if ideal transformer properties are assumed [25]. Therefore, if the respective winding currents are $\overline{I}_1$, $\overline{I}_2$ and $\overline{I}_3$, following relationship holds true,

$$N_1\overline{I}_1 + N_2\overline{I}_2 - N_3\overline{I}_3 = 0 \quad (12)$$

This relationship suggests that a magnetic core can couple multiple windings and operate them simultaneously to achieve a net result. If $N_1/N_3 = n_1$ and $N_2/N_3 = n_2$, where n_1 and n_2 are transformer turns ratios and $\overline{I}_3 = \overline{I}_s = I_L$, then (12) simplifies as below,

$$n_1\overline{I}_1 + n_2\overline{I}_2 = \overline{I}_L \quad (13)$$

As per Fig. 6(a), the relationships between the input, output voltages ($\overline{V}_{\text{in}}, \overline{V}_{\text{out}}$), the secondary voltage ($\overline{V}_{\text{s}}$), and the primary-1, primary-2 voltages ($\overline{V}_{\text{p1}}$, $\overline{V}_{\text{p2}}$) are given by,

$$\overline{V}_{\text{out}} = \overline{V}_{\text{in}} \pm \overline{V}_{\text{s}} \quad (14)$$

$$\overline{V}_{\text{a1}} = \overline{V}_{\text{in}} - \overline{V}_{\text{p1}}; \qquad \overline{V}_{\text{a2}} = \overline{V}_{\text{in}} - \overline{V}_{\text{p2}} \quad (15)$$

For achieving the results disclosed in section V of this paper, the winding turns ratios of two set of windings, n_1, n_2, are selected based on the case of maximum efficiency at the worst case input voltages given by (6).

In Fig. 6, switches S-1 and S-2 are used to alter the secondary windings' turn counts to change the active turns ratio as required by the boost- and buck-mode operation which are illustrated in Figs. 6(b) and (d). As indicated by the dots in transformer windings, secondary-2 induces a subtractive voltage, which opposes the polarity of the secondary-1 voltage. During buck-mode, as indicated in Fig. 6(d), this subtractive voltage maintains output regulation without driving transistor array into high impedance. And in the boost-mode, an additive voltage is induced in the combined secondary winding as indicated in Fig. 6(b). This arrangement can be used to achieve winding turns ratios according to the requirement using standard tapped transformers without the need to purchase customized transformers which adds an extra cost for manufacturing.

When the input line voltage falls within $\pm 2\%$ of the nominal voltage ($225-235$ V), the regulating circuit is bypassed by switch S-1 (see Fig. 6(c)), thus giving maximum efficiency. Switches S-3 and S-4 are used to disconnect the two arrays when they are not conducting.

Fig. 7 shows an implementation of a 230 V, 50 Hz multi-winding transformer regulator. This block diagram illustrates the key operations for RMS output voltage control:

(a) Feedback controller monitors the regulator output and produces the error signal that feeds the drive stage (see Fig. 2(c))
(b) Input sensing AC switch controller controls the $S_1 - S_4$ AC switches according to the regulator input voltage
(c) Optoisolator based drive stage drives the power transistor array according to the feedback signal to buffer the voltage difference between the output and the input
(d) Multi-winding transformer induces the correction voltage in the secondary winding as a result of effective impedance variation of the transistor array
(e) electrical isolation between the high power transistors and low power control circuit is achieved using a multi-stage optoisolator.

The authors have rebuilt the feedback controller used in the basic linear AC technique by adapting suitable modification to integrate with the multi-winding transformer design. The PIC microcontroller based control circuit is introduced to drive a set of AC switches which alter the transformer winding configuration based on the input voltage variations. This input sensing circuit is electrically isolated by the use of an optoisolator as indicated in Fig. 7.

For any general load connected at the regulator output, the regulated output voltage is given by,

$$\overline{V}_{\rm out} = \overline{V}_{\rm in}(1 + A/B) - \overline{I}_{\rm L}/B \qquad (16)$$

where, $A = n_1/Z_1 + n_2/Z_2 \quad B = n_1^2/Z_1 + n_2^2/Z_2$
Z_1 and Z_2 effective impedance of array-1 and array-2

The regulator efficiency is,

$$\eta = 1 - P_{\rm a1}/P_{\rm in} - P_{\rm a2}/P_{\rm in}, \qquad (17)$$

where $P_{\rm in}$ is the input power, and $P_{\rm a1}$, $P_{\rm a2}$ are instantaneous power dissipations in array-1 and array-2. Thus, minimizing array losses will optimize regulator efficiency.

IV. Equivalent Circuit Analysis of the Proposed Techniques

The equivalent circuit diagrams of the series dual-transformer and the multi-winding transformer configurations are shown in Figs. 8(a) and (b). Table II provides the parameters of 240 VA toroidal transformer using the measurements obtained by open and short circuit tests carried out at rated voltage and current of line-frequency (50 Hz) and referenced to the primary side [23, 24].

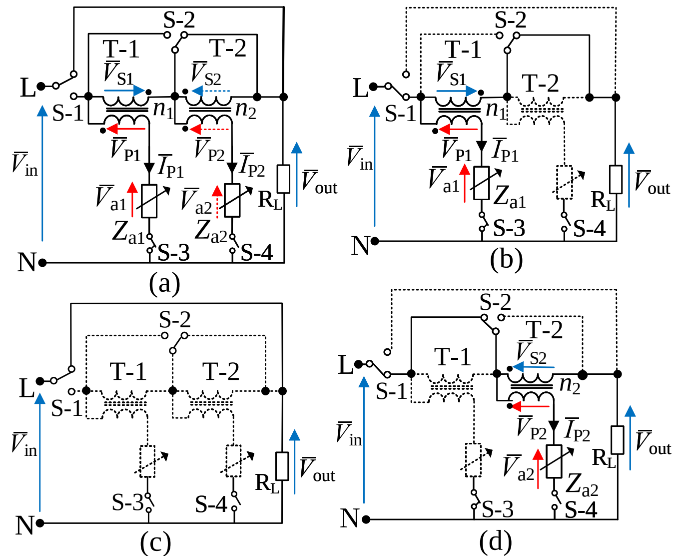

Fig. 5: Operational sequences of the power stage: Dual-transformer version (a) schematic diagram (b) T-1 at boost mode; (c) input reaches nominal voltage; (d) T-2 at buck mode

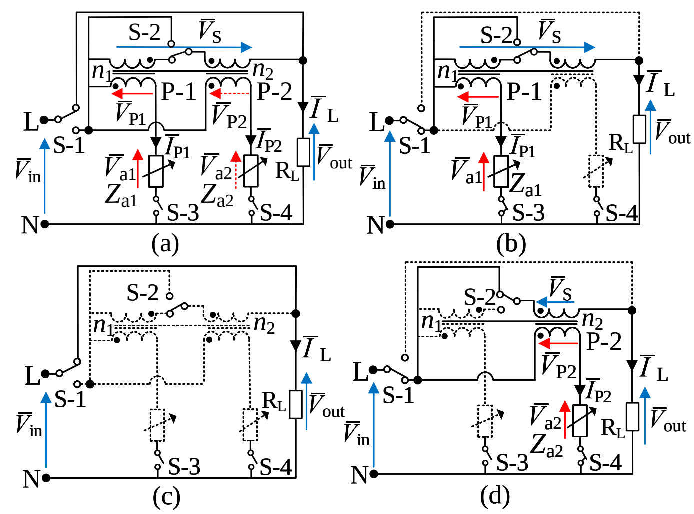

Fig. 6: Operational sequences of the power stage: Multi-winding version (a) schematic diagram (b) P-1 at boost mode; (c) input reaches nominal voltage; (d) P-2 at buck mode

Following Fig. 8, the basic relationships that govern the dual-transformer regulator using measured parameter values,

$$\overline{V}_{\rm in} = \overline{e}_{\rm p1} + \overline{I}_1(Z_{\rm a1} - Z_{\rm eq1}) \qquad (18)$$

$$\overline{V}_{\rm in} = \overline{e}_{\rm p2} + \overline{I}_2(Z_{\rm a2} - Z_{\rm eq2}) - \overline{e}_{\rm s1} \qquad (19)$$

where, $Z_{\rm eq} = R_{\rm eq} + jX_{\rm eq}$; and $X_{\rm eq} = 2\pi f L_{\rm eq}$

Assuming constant magnetizing impedance on loaded conditions, the induced primary voltage ($\overline{e}_{\rm p1}$) is given by,

$$|\overline{e}_{\rm p1}| = \overline{I}_{\rm e}\sqrt{\left(\frac{R_{\rm c1}^2 X_{\rm m1}}{R_{\rm c1}^2 + X_{\rm m1}^2}\right)^2 + \left(\frac{R_{\rm c1} X_{\rm m1}^2}{R_{\rm c1}^2 + X_{\rm m1}^2}\right)^2}$$

$$\angle e_{\rm p1} = \theta = \cos^{-1}\left(X_{\rm m1}/R_{\rm c1}\right) \qquad (20)$$

The regulator output voltage is given by,

$$\overline{V}_{\rm out} = \overline{V}_{\rm in} + \overline{e}_{\rm s1} \pm \overline{e}_{\rm s2} \qquad (21)$$

This article has been accepted for publication in a future issue of this journal, but has not been fully edited. Content may change prior to final publication. Citation information: DOI 10.1109/JESTIE.2020.3003350, IEEE Journal of Emerging and Selected Topics in Industrial Electronics

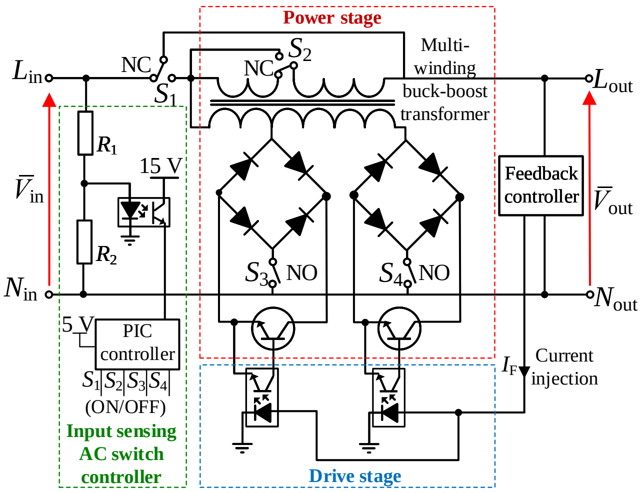

Fig. 7: Block diagram of multi-winding transformer regulator

TABLE II: Experimental measurements for transformer parameters of dual-transformer and multi-winding transformer regulators

Transformer parameters	Measured values: Two transformers T-1 (n=6.7)	T-2 (n=24)	Two windings W-1 (n=6.7)	W-2 (n=24)
Pri referred magnetizing inductance, L_M	43.4 H	52 H	43.4 H	44.3 H
Pri. referred core-loss, R_C	14.6 kΩ	17.1 kΩ	14.6 kΩ	20 kΩ
Eqv. leakage inductance, L_{eq}	10 mH	6.7 mH	10 mH	5.7 mH
Primary resistance, r_{p}	4 Ω	5.3 Ω	4 Ω	17 Ω
Secondary resistance, r_{s}	0.3 Ω	0.13 Ω	0.3 Ω	0.15 Ω
Excitation current, $\overline{I}_e$	21.2 mA	22 mA	21.2 mA	24 mA

According to Fig. 8(b), basic equations for the single-transformer multi-winding regulator using measured parameter values can be written as,

$$\overline{V}_{\text{out}} = \overline{V}_{\text{in}} \pm \overline{e}_{\text{s}} \tag{22}$$

$$\overline{V}_{\text{in}} = \overline{e}_{\text{p1}} + \overline{I}_1(Z_{\text{a1}} - Z_{\text{eq1}}) \tag{23}$$

$$\overline{V}_{\text{in}} = \overline{e}_{\text{p2}} + \overline{I}_2(Z_{\text{a2}} - Z_{\text{eq2}}) \tag{24}$$

Primary winding voltages $\overline{e}_{\text{p1}}$ and $\overline{e}_{\text{p2}}$ follows the general form given by Eq. (20).

Fig. 9(a) shows the efficiencies versus input voltage for the multi-winding case, comparing the measured efficiency versus the two calculated cases. In the graph showing highest performance, the transformer is treated as ideal. In the next case, where the transformer is treated as non-ideal, the efficiency was calculated based on transformer parameters shown in Table 2. Theoretical calculations are based on MATLAB R2017b software and the real and ideal case equivalent circuits were simulated and results were validated using LTSpice software. Measured efficiency curve indicates slightly lower values, due to measurement errors, secondary losses such as the PCB track losses and other connections.

V. Results

Fig. 9(b) compares the efficiencies of the multi-winding (Fig. 6) and dual-transformer designs (Fig. 5) with the original

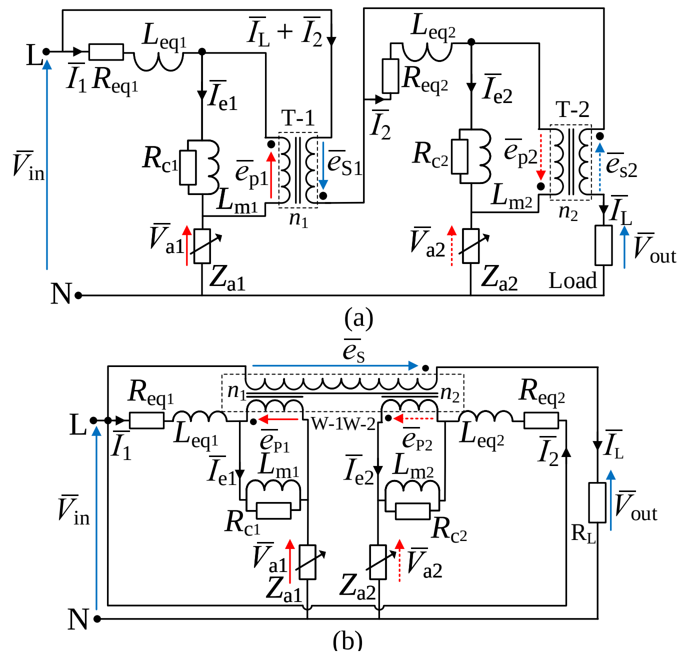

Fig. 8: Equivalent circuit diagrams; (a) dual-transformer regulator (b) single-transformer multi-winding transformer regulator

single-transformer configuration (Fig. 3). The data presented here are based on 230 V nominal output voltage.

As per the efficiency graph in Fig. 9(b), the curve of the original single transformer design has a diminishing profile at higher input voltages due to the significant power loss in the array.

In Fig. 9(c), the dual-transformer design shows an efficiency improvement at higher input voltages due to the action of the second transformer that governs the buck-mode regulation. Similarly in Fig. 9(d), the multi-winding approach exhibits an efficiency improvement at higher input voltages by shifting the operation of one primary winding to the other when the input voltage transits from boost to buck mode. The switching between windings is required only when the input voltage drops below the nominal or increases beyond nominal by more than $\pm 2\%$.

A set of oscillograms based on measurements using a Tektronix 2000 series oscilloscope is shown in Fig. 10. Each oscillogram displays voltage, current waveforms of input and output of three design configurations at $V_{\text{out}} = 230$ V and $I_{\text{L}} = 1.2$ A. In the single transformer design, a distorted output waveform is observed. This is because when the input voltage rises above nominal, the array is driven into very high impedance that makes the cross-over distortion and related non-linear effects of the transistors/diodes become more significant. A discussion on harmonic distortion due to these effects is beyond the scope of this paper and post graduate research work is in progress. The oscillogram in Fig. 10(d) illustrates the response time of the feedback circuit which is approximately 150 ms.

VI. Conclusion

This work indicates that the issue of lower efficiencies at input line voltages getting closer to the nominal line voltage

This article has been accepted for publication in a future issue of this journal, but has not been fully edited. Content may change prior to final publication. Citation information: DOI 10.1109/JESTIE.2020.3003350, IEEE Journal of Emerging and Selected Topics in Industrial Electronics

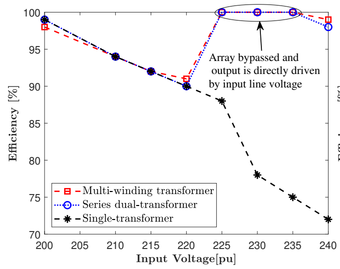

(a)

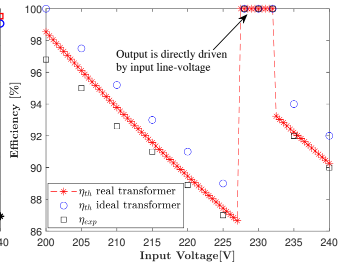

(b)

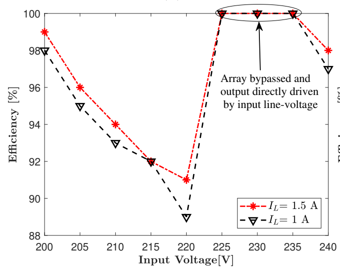

(c)

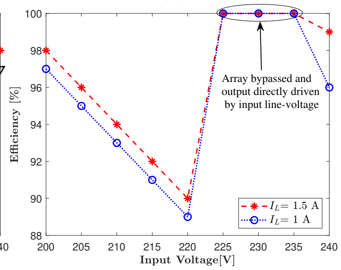

(d)

Fig. 9: Efficiency curves; (a) comparison of three designs; (b) experimental and calculated results of multi-winding design; (c) dual-transformer; (d) multi-winding transformer

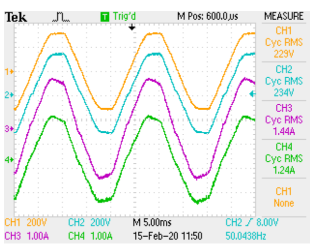

(a) Two-winding regulator

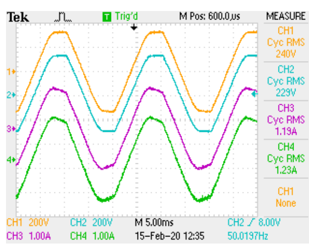

(b) Dual-transformer regulator

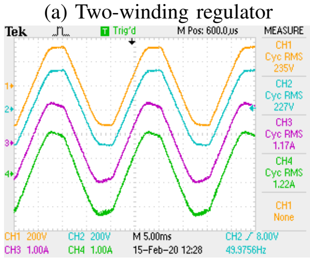

(c) Multi-winding regulator

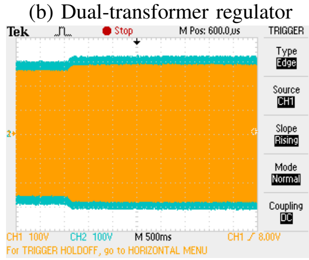

(d) Time-response of the control circuit

Fig. 10: Voltage and current waveforms of input and output; Yellow and purple - input parameters; blue and green- output parameters.

of the linear AC voltage regulator can be eliminated by the use of a single multi-winding buck-boost transformer, or a pair of transformers. Given that the power stage of this technique is based on simple lower cost line frequency transformers, we have shown that despite the use of a linear transistor circuit, it can cost effectively achieve the efficiencies typical to commercially implementable techniques, including the PWM techniques based switch-mode types.

Once commercial considerations related to low frequency line transformers are also taken into account, multi-winding case becomes more attractive, in single phase AC regulators in the range of 300 VA to 2 kVA.

References

[1] A. Bendre, D. Divan, W. Kranz, and W. Brumsickle, "Equipment failures caused by power quality disturbances," in *Industry Applications Conference, 39th IAS Annual Meeting. Conference Record of the IEEE*, vol. 1, (Seattle), 2004.

[2] "What is power quality?," technical report, Electric Power Research Institute), 2004.

[3] "IEEE recommended practice for monitoring electric power quality (IEEE std 1159-2019)," standard, IEEE Power and Energy Society, 2019.

[4] N. A. D. V. Kularatna and M. D. C. S. K. Jinadasa, "Digital control for controlling and linearizing an AC impedance," 2015, Sep.15.

[5] N. Kularatna, "A linear technique for AC voltage regulation using an ordinary transformer and power semiconductors," 1990.

[6] P. N. Wijesooriya, N. Kularatna, J. Fernando, and D. A. Steyn-Ross, "Two-transformer-series approach in developing a transistor based-AC voltage regulator for consumer-end applications," in *43rd Annual Conference of the IEEE Industrial Electronics Society (IECON)*, (Beijing, China), pp. 6437–6442, 2017.

[7] P. N. Wijesooriya, N. Kularatna, and D. A. Steyn-Ross, "Use of multiple transformer windings for efficiency enhancement in the series transistor-array based linear AC voltage regulator," in *Applied Power Electronics Conference and Exposition (APEC)*, (Anaheim, CA, USA), pp. 2414–2419, 2019.

[8] P. Nystrom, "A comparison of AC voltage regulation technologies," tech. rep., Tsi Power, June 2012.

[9] P. Eswaran and M. Nishanth, "Design of fuzzy logic controller for customized servo voltage stabilizer," in *2nd International Conference on Electronics and Communication Systems (ICECS)*, (Coimbatore), pp. 103–106, Feb 2015.

[10] M. G. Lind, W. Xiao, and W. G. Dunford, "Modeling of a constant voltage transformer," *IEEE Transactions on Circuits and Systems I: Regular Papers*, vol. 53, no. 2, pp. 409–418, 2006.

[11] M. M. Hoque, "Design, implementation and performance study of programmable automatic voltage regulator," *Journal of Electrical Systems*, vol. 10, no. 4, 2014.

[12] M. Ali, N. Anwar, S. T. Zahra, A. Hayat, S. Zaffar, and S. Iqbal, "Triac based automatic voltage stabilizer," *University of Wah Journal of Science and Technology (UWJST)*, vol. 3, pp. 23–28, 2019.

[13] M. Hajimoradi, E. Karimi, H. Mokhtari, and A. Yazdian, "Performance improvement of a double stage switch mode AC voltage regulator," in *3rd conference on Power Electronics and Drive Systems Technology (PEDSTC)*, (Tehran, Iran), pp. 181–186, 2012.

[14] D. Chen and Y. Chen, "Step-up ac voltage regulators with high-frequency link," *IEEE transactions on power electronics*, vol. 28, no. 1, pp. 390–397, 2012.

[15] C. Jiong, Z. Feng, C. Xia, Z. Lizhi, and W. Luyang, "Design of ac chopper voltage regulator based on PIC16F716 microcontroller," in *IEEE PES Innovative Smart Grid Technologies*, (Tianjin), pp. 1–4, 2012.

[16] J. Nan, T. Hou-Jun, L.-Y. Bai, X. Geng, and X.-L. Yang, "Analysis and control of two switches ac voltage regulator," vol. 9, pp. 208–217, April 2010.

[17] C.-M. Wang, C.-H. Lin, C.-H. Su, and S.-Y. Chang, "A novel single-phase soft-switching ac chopper without auxiliary switches," *IEEE transactions on power electronics*, vol. 26, no. 7, pp. 2041–2048, 2010.

[18] T. Tomioka, "Voltage regulator and semiconductor device," Oct. 24 2017. US Patent 9,798,341.

[19] P. Banerjee, M. Choudhury, and G. T. Rasul, "Ac voltage regulation by switch mode buck-boost voltage controller," in *3rd Int. Confonf. ICECE, Bangladesh*, pp. 351–354, 2004.

[20] N. Kularatna and C. Jinadasa, "Analysis and design aspects of a series power semiconductor array with digital waveform control capability for single phase AC voltage regulators and other applications," *Circuits and Systems*, vol. 2, no. 3, p. 249, 2011.

[21] F. Vandy, "Design and implementation of an AC voltage regulator based on series power semiconductor array," 2014.

[22] N. Kularatna, "Low cost, light weight AC regulator employing bipolar power transistors," in *Proceedings of the 21st International Power Quality Conference-PCIM/Power Quality*, vol. 90, pp. 67–76, 1990.

[23] C. W. T. McLyman, *Transformer and inductor design handbook*. CRC press, 2016.

[24] J. H. Harlow, *Electric Power Transformer Engineering, 3rd edition*. Taylor and Francis, 2012.

[25] V. C. Valchev and A. Van den Bossche, *Inductors and transformers for power electronics*. CRC press, 2005.